XLI CILAMCE
XLI Ibero-Latin American Congress on Computational Methods in Engineering
16-19 November, 2020 FOZ DO IGUAÇU PARANÁ - BRAZIL

Nonlinear Acoustic Wave Propagation in Stratified Media

F. P. Piccoli[1], L. C. de Jesus[1], J. T. A. Chacaltana[1]

[1]*Free-Surface Flow Laboratory (LABESUL), Dept. of Environmental Engineering, Federal University of Espírito Santo.*
Av. Fernando Ferrari, 514, Goiabeiras, Vitória, 29075-910, Espírito Santo, Brazil
fabio.p.piccoli@gmail.com

Abstract. The acoustic waves propagation is a subject of great application in several areas of engineering, for example in marine seismic for the detection of underwater objects, in hydrography and navigation for the detection of the seabed, among others. In this work, a nonlinear model for the propagation of P-waves in a stratified environment is developed. Starting from the nonlinear equations that governs the fluid motion of a compressible fluid with mass source we obtain the nonlinear equations for the acoustic P-wave propagation. The set of equations in the conservative form are solved numerically using the finite difference method applying the explicit strong stability-preserving (SSP) multistep method. In order to achieve higher order accuracy in time, the fourth-order SSP Runge–Kutta time discretization was implemented and the Courant-Friedrichs-Levy (CFL) criterion must be satisfied for an adaptative time step along the simulation. The second order spatial derivatives are solved using the minmod based MUSCL spatial discretization. A numerical code is written in Fortran language and simulations with a Ricker-type pressure source were performed. Numerical results are in good agreement with those reported in the literature.

Keywords: Seismic waves, numerical modeling, marine geophysics.

1 Introduction

The numerical study of the propagation of acoustic waves is a subject of great interest in the area of geophysics. The applications of these waves in heterogeneous media cause discontinuities in physical properties, in which the numerical methods are an excellent tool for studying the propagation of acoustic waves in large dimensions and with satisfactory results for understanding the acoustic behavior in water and in substrates (Antunes [1]).

Research on seismic waves and propagation is a first step in understanding the material characteristics (e.g. sedimentary pattern, type of sediment, presence of oil, salt domes, among others) and the exploration by the oil and gas industry. A typical understanding of the seismic waves, consists of the generation of an acoustic wave that propagates in different sedimentary layers. Generally, this acoustic wave or seismic wave propagates from the source on the water surface to the different sedimentary layers. Propagating in different layers the acoustic wave may be refracted, diffracted and / or reflected. These effects can be recorded by geophones, which record the time series of the reflect waves that are called seismic traces or seismogram. Thus, the numerical modeling of the acoustic wave is a valuable tool for the interpretation, evaluation and design of seismic equipment (Abdelkhalek [2]).

Much of the research on acoustic or seismic waves modeling assume that the Pressure field is expressed by the scalar wave equation, where it is represented by the second derivative operator in the time of the pressure and by the Laplacian operator of the pressure in space (e.g. Santos [3]; Fernandes [4]; Wang [5]; Xu [6]). Generally, the finite difference method is used to solve the spatial derivatives of the Laplacian operator (Xu [6]).

In this paper a nonlinear numerical model for the propagation of the seismic waves was developed. The numerical theory was based following the work of Shi [7] and Liu [8], in which was developed an algorithm using a hybrid TVD finite-difference and finite-volume method for the set of nonlinear equations. This technique provides fast and accurate simulation and was applied in several case studies with wave-speed domains stratified.

2 Nonlinear Seismic Wave Equations

The nonlinear acoustic wave model was developed from the Mass and Momentum Conservation Laws for a compressible fluid. We applied the concept of dimensional analysis to the Momentum equation and combine the elasticity-modulus equation with the mass conservation to obtain a closed set of equations for the pressure (P) e velocity ($\vec{u}$). The resulting nonlinear equations are written in a conservative form to facilitate the numerical implementation of the methodology used in this paper. For simplicity, the acoustic wave equations are written in the dimensionless variables $P' = P/E$, considering $E \neq E(t)$ and $E = E(x, y)$, where $E = \rho(DP/Dt)/(D\rho/Dt)$ is the modulus of elasticity of the medium. The resulting set of equation to simulate the P-waves propagation as a function of time (t) are given by

$$\frac{\partial P'}{\partial t} + \nabla.[1 + P')\vec{u}] = \dot{P}_f(t) + P'(\nabla.\vec{u} - \vec{u}.\frac{\nabla E}{E}) \tag{1}$$

$$\frac{\partial \vec{u}}{\partial t} + \nabla.(\vec{u}\vec{u}) + \nabla(c^2 P') = \vec{u}(\nabla.\vec{u}) + 2P'c\nabla c - \frac{c^2 P'}{E}\nabla E \tag{2}$$

where ∇ is the differential nabla operator $(\partial/\partial\, x, \partial/\partial\, y)$ in the horizontal coordinates (x) and vertical coordinates (y), $\vec{u}$ is the velocity vector (u, v) and c is the wave speed (celerity) in the medium. The relation of modulus of elasticity with the celerity is $E = \rho c^2$, where ρ is the density of medium. $\dot{P}_f(t)$ is the pressure source term determined by the first derivative of a Gaussian function (Ricker-type pressure source by Moreira [9]) given by

$$\dot{P}_f(t) = t_0 \exp(-0.25\pi f_c^2 t_0^2) \tag{3}$$

in which $f_c = 3\sqrt{f}$ is the central frequency of the source and f is the cutoff frequency. $t_0 = \mathrm{t} - 2\sqrt{\pi}/f$ is the time required to guarantee $\dot{P}_f(t) = 0$ for $t < 0$.

3 Numerical Scheme

The generalized and compact form of eq. (1) and eq. (2) can be defined as

$$\partial\boldsymbol{\psi}/\partial t + \nabla.\boldsymbol{\phi}(\boldsymbol{\psi}) = \boldsymbol{S} \text{ where, } \boldsymbol{\psi} = \begin{pmatrix} P' \\ u \\ v \end{pmatrix} \text{ and } \boldsymbol{\phi} = \begin{pmatrix} (1+P')(u\boldsymbol{i} + v\boldsymbol{j}) \\ (uu + c^2P')\boldsymbol{i} + (uv)\boldsymbol{j} \\ (vu)\boldsymbol{i} + (vv + c^2P')\boldsymbol{j} \end{pmatrix} \tag{4}$$

$$\boldsymbol{S} = \begin{pmatrix} \dot{P}_f(t) + P'(\partial u/\partial x + \partial v/\partial y\ - uE^{-1}\partial E/\partial x - vE^{-1}\partial E/\partial y) \\ u(\partial u/\partial x + \partial v/\partial y) + cP'(2\partial c/\partial x - cE^{-1}\partial E/\partial x) \\ v(\partial u/\partial x + \partial v/\partial y) + cP'(2\partial c/\partial y - cE^{-1}\partial E/\partial y) \end{pmatrix} \tag{5}$$

Thus, the dimensional pressure value can be obtained by $P = P'E$.

The numerical scheme developed consists of a combined finite-volumes/finite-differences method, as presented in Shi [7] for gravity waves. This method has two main steps to solve the numerical fluxes $\nabla.\boldsymbol{\phi}(\boldsymbol{\psi})$ of the acoustic wave equation: the first step is to use the reconstruction technique to calculate the values at the numerical grid cell interface; The second step uses the local Riemann solver to predict the fluxes at the grid cell interfaces. The acoustic wave equation dispersive terms $\boldsymbol{S}$ are solved by a 4th order finite difference method with 5 grid points.

The high-order MUSCL-TVD (Monotonic Upstream-centered Scheme for Conservation Laws - Total Variation Diminishing) was used to solve the flux terms and first order derivative terms. This technique is able to substantially reduce the numerical diffusion without causing non-physical oscillations (numerical noises), by linearly reconstructing the values of the flux variables within or at the cell interfaces (Hou [10]).

As in Liu [8], the modified MUSCL-TVD fourth-order scheme with the van-Leer Limiter (Erduran [11]) is used to obtain the values of conservative variables at the cell interfaces, following an HLL (Harten-Lax-Leer) approximation for the Riemann solver to obtain the fluxes (Harten [12]).

The combined form of the cell interface construction in the x direction can be written as

$$\phi^{L}_{i+\frac{1}{2}} = \phi_i + \frac{1}{4}\left[(1-\kappa_1)\chi(r)\Delta^*\phi_{i-\frac{1}{2}} + (1+\kappa_1)\chi\left(\frac{1}{r}\right)\Delta^*\phi_{i+\frac{1}{2}}\right] \tag{6}$$

$$\phi^{R}_{i-\frac{1}{2}} = \phi_i - \frac{1}{4}\left[(1+\kappa_1)\chi(r)\Delta^*\phi_{i-\frac{1}{2}} + (1-\kappa_1)\chi\left(\frac{1}{r}\right)\Delta^*\phi_{i+\frac{1}{2}}\right] \tag{7}$$

where $\phi^{L}_{i+1/2}$ is the value constructed on the left side of the $i+1/2$ interface and $\phi^{R}_{i-1/2}$ is the value constructed on the right side of the $i-1/2$ interface. The values of $\Delta^*\phi$ are as follows

$$\begin{aligned}
\Delta^*\phi_{i+\frac{1}{2}} &= \Delta\phi_{i+\frac{1}{2}} - \kappa_2\left(\Delta^3\bar{\phi}_{i+\frac{1}{2}}\right)/6 \\
\Delta\phi_{i+\frac{1}{2}} &= \phi_{i+1} - \phi_i \\
\Delta^3\bar{\phi}_{i+\frac{1}{2}} &= \Delta\bar{\phi}_{i+\frac{3}{2}} - 2\Delta\bar{\phi}_{i+\frac{1}{2}} + \Delta\bar{\phi}_{i-\frac{1}{2}} \\
\Delta\bar{\phi}_{i-\frac{1}{2}} &= \text{minmod}\left(\Delta\phi_{\text{i}-\frac{1}{2}}, \Delta\phi_{i+\frac{1}{2}}, \Delta\phi_{i+\frac{3}{2}}\right) \\
\Delta\bar{\phi}_{i+\frac{1}{2}} &= \text{minmod}\left(\Delta\phi_{\text{i}+\frac{1}{2}}, \Delta\phi_{i+\frac{3}{2}}, \Delta\phi_{i-\frac{3}{2}}\right) \\
\Delta\bar{\phi}_{i+\frac{3}{2}} &= \text{minmod}\left(\Delta\phi_{\text{i}+\frac{3}{2}}, \Delta\phi_{i-\frac{1}{2}}, \Delta\phi_{i+\frac{1}{2}}\right)
\end{aligned} \tag{8}$$

In eq. (8), minmod represents the MinMod Limiter, which selects the lowest value in modulus if its arguments have the same sign, and zero if its arguments have different sign. This function ensures that in regions of maximum and minimum the local diffusive flux will be null, making the numerical flow of the first order, preventing spurious oscillations in the solution. Thus, the MinMod Limiter for variables (a, b, c), for example, is given by

$$\text{minmod}(a, \text{b}, \text{c}) = \text{sign}(a)\,\max\{0, \min[|a|, 2\text{sign}(a)b, 2\text{sign}(a)c]\} \tag{9}$$

κ_1 in eq. (6) and eq. (7), and κ_2 in eq. (8) are control parameters for orders of the scheme in the compact form. For fourth order it is used $(\kappa_1, \kappa_2) = (1/3, 1)$, for third order it is used $(\kappa_1, \kappa_2) = (1/3, 0)$ and for second order it is used $(\kappa_1, \kappa_2) = (-1, 0)$. The term $\chi(r)$ in eq. (6) and eq. (7) is the van-Leer limiter and can be expressed as

$$\chi(\text{r}) = \frac{\text{r} + |\text{r}|}{1 + \text{r}} \quad \text{where} \quad \text{r} = \frac{\Delta^*\phi_{i+\frac{1}{2}}}{\Delta^*\phi_{i-\frac{1}{2}}} \tag{10}$$

Thus, numerical fluxes are calculated using an HLL approximation for the Riemann solver

$$\boldsymbol{\phi}(\boldsymbol{\psi^L}, \boldsymbol{\psi^R}) = \begin{cases} \boldsymbol{\phi}(\boldsymbol{\psi^L}) & \text{if } \text{S}_\text{L} \geq 0 \\ \boldsymbol{\phi}^*(\boldsymbol{\psi^L}, \boldsymbol{\psi^R}) & \text{if } \text{S}_\text{L} < 0 < S_R \\ \boldsymbol{\phi}(\boldsymbol{\psi^R}) & \text{if } \text{S}_\text{R} \leq 0 \end{cases} \tag{11}$$

The wave velocities of the Riemann solver on the cell faces (S_L and S_R) are given by

$$S_L = \min(\vec{u}^L \cdot \boldsymbol{n} - C^L, u^* - \sqrt{\varphi^*}) \tag{12}$$

$$S_R = \max(\vec{u}^R \cdot \boldsymbol{n} + C^R, u^* + \sqrt{\varphi^*}) \tag{13}$$

where u^* and φ^* are estimated as:

$$u^* = \frac{1}{2}(\vec{u}^R + \vec{u}^L) \cdot \boldsymbol{n} + c^L - c^R \quad \text{and} \quad \sqrt{\varphi^*} = \frac{c^L + c^R}{2} + \frac{(\vec{u}^R + \vec{u}^L) \cdot \boldsymbol{n}}{4} \tag{14}$$

where $\boldsymbol{n}$ is the normal vector at the face of the cell and (c^L, c^R) are the wave speed calculated at the left and right interfaces of the cell, respectively. In the y direction it follows the same procedure, where the sub-index i becomes

j and the cell faces are the top (T) and bottom (B).

The temporal integration methods used in the acoustic wave model are based on the Runge-Kutta methods modified by Gottlieb [13]. This method consists of the third order approximation to preserve the stability of the Runge-Kutta scheme (Strong Stability-Preserving - SSP). Thus, we have

$$\boldsymbol{\psi}^{(1)} = \boldsymbol{\psi}^{(n)} + \Delta t\left(-\nabla \cdot \boldsymbol{\phi}\left(\boldsymbol{\psi}^{(\mathrm{n})}\right) + \boldsymbol{S}^{(1)}\right) \tag{15}$$

$$\boldsymbol{\psi}^{(2)} = \frac{3}{4}\boldsymbol{\psi}^{(n)} + \frac{1}{4}\left[\boldsymbol{\psi}^{(1)} + \Delta t\left(-\nabla \cdot \boldsymbol{\phi}\left(\boldsymbol{\psi}^{(1)}\right) + \boldsymbol{S}^{(2)}\right)\right] \tag{16}$$

$$\boldsymbol{\psi}^{(n+1)} = \frac{1}{3}\boldsymbol{\psi}^{(n)} + \frac{2}{3}\left[\boldsymbol{\psi}^{(2)} + \Delta t\left(-\nabla \cdot \boldsymbol{\phi}\left(\boldsymbol{\psi}^{(2)}\right) + \boldsymbol{S}^{(n+1)}\right)\right] \tag{17}$$

where the superscript n indicates the present time level and the superscripts (1) and (2) indicate the intermediate stages of the Runge-Kutta multistep integration. For efficiency in numerical stability of the acoustic wave model, the model was implemented following the Shi [7] and Liu [8] method for gravity waves using an adaptive time step (Δt), following the Courant-Friedrichs-Lewy (CFL) criterion

$$\Delta t = Crmin\left[min\left(\frac{\Delta x}{|u_{i,J}| + c}\right), min\left(\frac{\Delta y}{|v_{I,j}| + c}\right)\right] \tag{18}$$

where Cr is the Courant number and c is the acoustic wave celerity.

When the wave reaches a solid wall, it will be reflected completely. For a fully reflective boundary condition with a normal vector to wall $\boldsymbol{n}$, the boundary conditions are given by

$$\vec{u} \cdot \boldsymbol{n} = 0 \text{ and } \nabla P \cdot \boldsymbol{n} = 0 \tag{19}$$

For the Absorbing Boundary Condition (ABC) the method found in Cerjan [14] was used. In this method, the variables $\boldsymbol{\psi}$ are gradually reduced after each time step until reaches zero in the numerical grid boundaries. The equations for this attenuation is given by

$$\boldsymbol{\psi} = \boldsymbol{\psi} e^{-[\gamma_{nbc}(n_{nbc} - d_{nbc})]^2} \tag{20}$$

where γ_{nbc} is a damping factor, n_{nbc} is the number of points used for the damping layer and i_{nbc} is the number of points in a position (i, j) of the boundary.

4 Results e Discussion

4.1 Case Study of Reflective and ABC Conditions

This case represents the propagation of an acoustic wave with a cutoff frequency of $40Hz$ located in the center of a $300m \times 500m$ rectangular domain. The cells of the computational mesh have homogeneous faces with $1m$ edges, totaling 300×500 cells from the computational domain. Two simulations were performed, the first with reflection in all grid boundaries and the later with absorbing only on the sides of the boundary. The wave speed and density are considered homogeneous in the whole domain, with values of $1400m/s$ and $1000kg/m^3$. Respectively. For the time discretization, a CFL value of 0.5 was used, with a total simulation time of $1.0s$.

Figure 1 show the results of the simulation for fully reflective condition – Fig.1a and ABC condition – Fig. 1b, comparing with the results of Santos [15]. The results showed that the absorbing boundary conditions were effective in the treatment of reflections caused by the boundaries of the numerical domain. The need to significantly extend the numerical domain to represent the domain of interest is reduced using this boundary condition. As the implemented algorithm adds virtual cells to the ABC layers, the domain is visualized as if it were with open boundary. For this example, 50 virtual cells were added to each boundary.

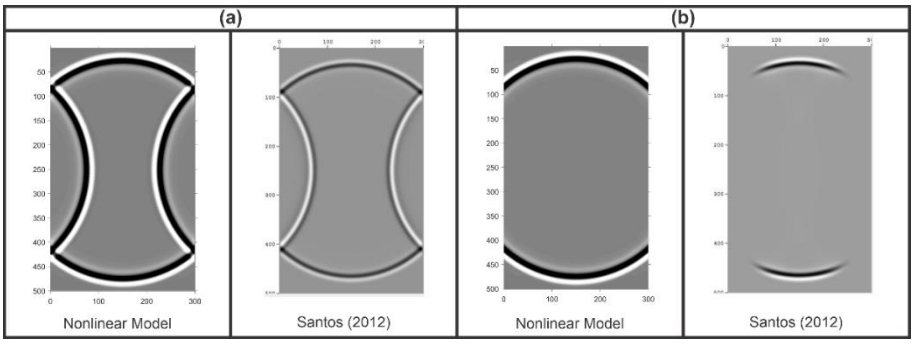

Figure 1. Snapshots of the different boundary conditions, (a) represents the fully reflective condition and (b) the ABC condition. The results are compared with those obtained by Santos [15].

4.2 Schematic geological structures

This case study consists of several domains with layers of different wave speeds (Santos [3]). These schemes represent the propagation of an acoustic wave with a cutoff frequency of $80Hz$ located at the coordinates $(x, y) = (550m, 0m)$. The cells of the computational mesh have faces with $2m$ edges, totalizing 550×300 cells of computational grid. In the domain boundaries, non-reflective boundary conditions (ABC) were applied. The wave speed varies from $2000m/s$ to $4000m/s$, with a homogeneous density of $1000kg/m^3$. For the time discretization, a CFL value of 0.5 was used to calculate the time step, with a total simulation time of $0.5s$. Figure 2 shows the schematic model for all cases to study with hypothetical geological basins. Figure 2a, represents a domain with two layers of different wave speeds, Fig. 2b shows a stratified wave speed field separated into 4 layers with a rectangular high speed wave intrusion at the center of the domain, Fig. 2c represents a schematic geological fault and the Fig. 2d show a geological basin with different acoustic wave speeds.

The synthetic seismogram calculated from the model results are shown in the second column of the Fig. 2. In the Fig. 2e, the reflections produced by the interfaces of different wave speeds are clearly reproduced by the acoustic wave model developed in this work. In the seismogram shown in the Fig. 2f, the events caused by the high-speed intrusion are clearly identified. This example is important because it is possible to detect domes of different materials along the depth of the substrate. In the Fig. 2g the representations of the schematic geological faults are identified in the seismogram, where inclined portions generate reflected regions with asymmetric intensity in the seismogram. In the Fig. 2h, the schematic geological basin is clear from the reflections captured by the synthetic seismogram.

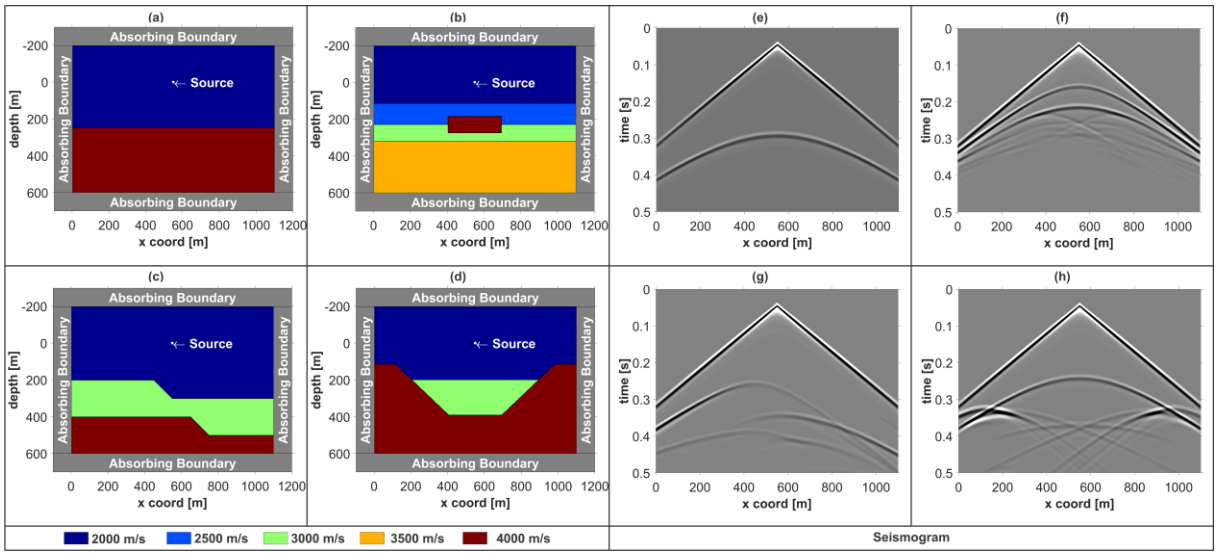

Figure 2. Domains with different acoustic wave speeds for testing the numerical model.

4.3 Salt Dome Model

This example uses data published by Bulant [16], a case study from Hess Corporation, which consists of a stratified domain for acoustic wave speeds and with a body of salt with constant acoustic wave speed (Fig. 3). The data were interpolated to a computational grid with 712×520 cells with $20m$ edges. The acoustic pulse was located at $(x, y) = (5000,0)m$ coordinates with a cut-off frequency of $20Hz$. The total simulation time was $6s$ with a CFL of 0.5, time needed for the wave to propagate and reflect in all layers of the domain. The source is generated in a medium with characteristic water acoustic wave speed ($\sim 1500m/s$) and the pulse is directed to the substrate with different layers of wave speed ($1500m/s < c < 3000m/s$), the highest acoustic wave speed being located in the Salt Dome ($> 4500m/s$).

The seismogram of the modeling results (Fig. 4) shows the reflections generated in the substrate layers, pointing to a greater intensity of reflection recorded around $3.5s$, referring to the reflection of the dome recorded by the geophone. Figure 4 also shows 4 snapshots referring to the propagation of the acoustic wave from the generation point to the return of the wave reflected by the dome. In snapshots of the Fig. 4 we observed an agreement with wave reflected by the salt dome and the seismogram.

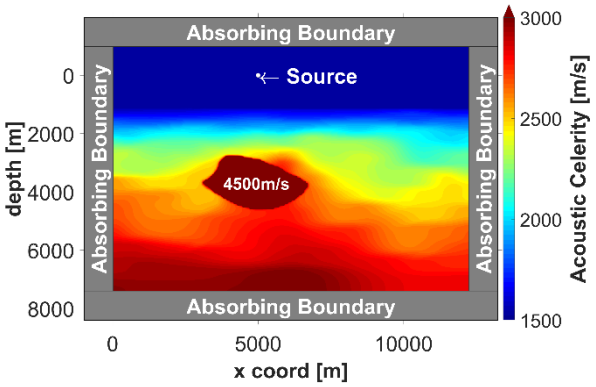

Figure 3. Acoustic wave speed field for a salt dome case. Model from Hess Corporation. Source: Bulant (2000).

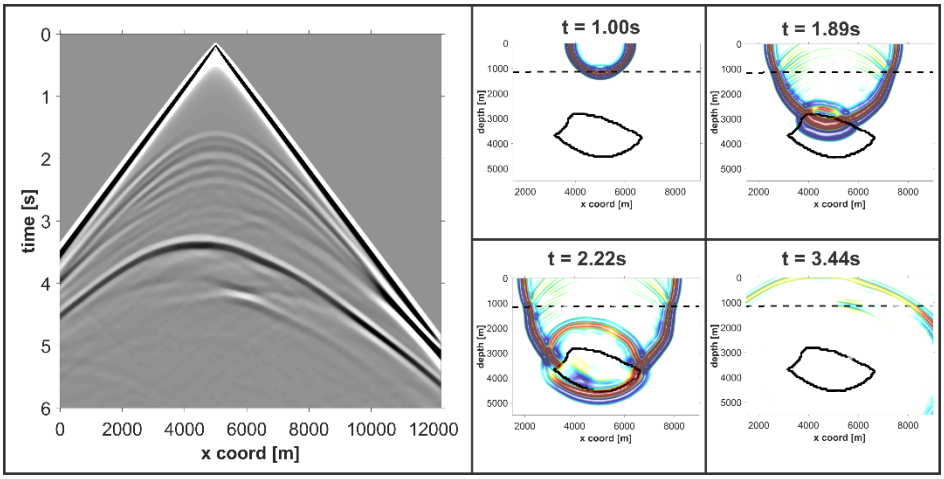

Figure 4. Seismogram, larger graphic on the left, and snapshots of the P-wave, small graphics on the right, of the results of the non-linear model for the salt dome of Hess corporation (Bulant [16]). The dashed line represents the variation of the wave speed between water and substrate and the continuous line indicates the position of the salt dome.

5 Conclusion

In this work, a nonlinear model of acoustic waves was developed using a hybrid technique of finite volumes and finite differences, adapted from a gravity wave model (Shi [7]). The model has good numerical stability, where the stability criteria (CFL) was used to calculate the variable time step for the simulation, allowing less computational time for the simulations. The MUSCL-TVD method with Riemann and HLL solver improved the

results, enabling the reduction of numerical noises generally generated by finite difference techniques with first order derivatives, without the need for numerical filters.

Several acoustic wave modeling studies use the second derivative of a Gaussian function as the generating source, due to the second derivative nature of the mathematical formulation of the pressure wave. Here, approximations of the acoustic wave were used in the Navier-Stokes equations, where the mathematical formulation presents a set of equations based on the Laws of Conservation of mass and Momentum. Thus, the source term used was the first derivative of a Gaussian function in time. The generating source shown a good behavior in comparison with the literature, however there is still a need for a better formulation in future works for the generating source in this system of equations.

The results of the simulation of the nonlinear model of acoustic waves, proved to be consistent and with a good qualitative representation of the tested cases with the identification of the main physical effects caused on the wave behavior along vertical layers of different materials (different wave speeds). For future work, it is important to implement the Reverse Time Migration (RTM) technique to generate the substrate imaging and, thus, determine the configuration of the vertical layers of the physical domain.

Acknowledgements. The authors from Espírito Santo Federal University acknowledge the financial support from Centro de Pesquisas Leopoldo Américo Miguez de Mello (CENPES/PETROBRAS), the Brazilian state oil company. The referees' comments are gratefully appreciated.

Authorship statement. The authors hereby confirm that they are the sole liable persons responsible for the authorship of this work, and that all material that has been herein included as part of the present paper is either the property (and authorship) of the authors, or has the permission of the owners to be included here.

References

[1] A. J. M. Antunes, R. C. P. Leal-Toledo, O. T. da Silveira Filho and E. M. Toledo. "Método de diferenças finitas para a equação de onda acústica utilizando passos de tempo ajustados localmente". *XI Simpósio de Mecânica Computacional, II Encontro Mineiro de Modelagem Computacional,* Juíz de Fora, Minas Gerais, Brazil, 2014.
[2] R. Abdelkhalek, O. C. J. Roman and G. Latu. "Fast Seismic Modeling and Reverse Time Migration on a GPU Cluster". *International Conference on High Performance Computing & Simulation*, pp. 36-46, 2009.
[3] R. H. M. dos Santos and W. M. Figueiró. "Modelagem Acústica Bidimensional usando diferentes parametrizações de campos de velocidades". *Revista Brasileira de Geofísica*,vol. 24, n. 1, pp. 103-115, 2006.
[4] L. L. Fernandes, J. C. R. Cruz, C. J. C. Blanco and A. R. B. Barp. "Modelagem Sísmica via Métodos das Diferenças Finitas – Caso da Bacia do Amazonas". *Acta Amazonica*, vol. 39, n. 1, pp. 155-164, 2009.
[5] Y. Wang and W. Liang. "Optimized Finite Difference Methods for Seismic Acoustic Wave Modeling". In: M. Reyhanoglu (ed.), *Computational an Experimental Studies of Acoustic Waves*, 2017.
[6] S. Xu and Y. Liu. "3D acoustic wave modeling with a time-space-domain temporal high-order finite-difference scheme". *Journal of Geophysics and Engineering*, vol. 15, pp. 1963-1976, 2018.
[7] F. Shi, J. T. Kirby, J. C. Harris, J. D. Geiman and S. T. Grili. "A high-order adaptive time-stepping TVD solver for Boussinesq modeling of breaking waves and coastal inundation". *Ocean Modelling*, vol. 43, n. 44, pp. 36-51, 2012.
[8] W. Liu, Y. Ning, F. Shi and Z. Sun. "A 2DH fully dispersive and weakly nonlinear Boussinesq-type model based on a finite-volume and finite-difference TVD-type scheme". *Ocean Modeling*, vol. 147, pp. 1-10, 2020.
[9] R. M. Moreira, M. A. C. Santos, J. L. Martins, D. L. F. Silva, R. B. V. Pessolani, D. M. S. Filho and A. Bulcão. "Frequency-domain acoustic-wave modeling with hybrid absorbing boundary conditions". *Geophysics*, vol.79, n; 5, pp. A39-A44, 2014.
[10] J. Hou, Q. Liang, H. Zhang and R. Hinkelmann. "An efficient unstructured MUSCL scheme for solving the 2D shallow water equations". *Environmental Modelling & Software*, vol. 66, pp. 131-152, 2015.
[11] K. S. Erduran, S. Ilic and V. Kutija. "Hybrid finite-volume finite-difference scheme for the solution of Boussinesq equations". *International Journal for Numerical Methods in Fluids*, vol. 49, pp. 1213-1232, 2005.
[12] A. Harten, P. D. Lax and B. van Leer. "On upstream differencing and Godunov-type schemes for hyperbolic conservation laws". *Society for Industrial and Applied Mathematics*, vol. 25, n. 1, pp. 35-61, 1983.
[13] S. Gottlieb, C.-W. Shu and E. Tadmor. "Strong Stability-Preserving High-Order Time Discretization Methods". *Society for Industrial and Applied Mathematics*, vol.43, n. 1, pp. 89-112, 2001.
[14] C. Cerjan, D. Kosloff, R. Kosloff and M. Reshef. "A nonreflecting boundary condition for discrete acoustic and elastic wave equations". *Geophysics*, vol. 50, n. 4, pp. 705-708, 1985.
[15] J. L. R. dos Santos. "Modelagem da Equação da Onda Acústica Aplicada ao Imageamento de Estruturas Geológicas". *Master Thesis, COPPE, Federal University of Rio de Janeiro*, Rio de Janeiro, Brazil, 2012. Retrieved: http://www.coc.ufrj.br/pt/documents2/mestrado/2012-2/2306-jorge-luiz-rebelo-dos-santos-mestrado/file.
[16] P. Bulant. "Smoothing 2-D model Hess for Kirchhoff migrations". In: Seismic Waves in Complex 3-D Structures, Report 10, pp. 75-82, 2000. Retrieved: http://sw3d.mff.cuni.cz/papers/r10pb100.htm.